J Appl Phycol (2010) 22:479–488
DOI 10.1007/s10811-009-9482-1

Toxic effects of antimony on photosystem II of *Synechocystis* sp. as probed by in vivo chlorophyll fluorescence

Daoyong Zhang · Xiangliang Pan · Guijin Mu · Jianlong Wang

Received: 23 October 2008 / Revised and accepted: 30 October 2009 / Published online: 28 November 2009

Abstract It has been demonstrated that antimony (Sb) at concentrations ranging from 1.0 to 10.0 mg L^{-1} inhibits O_2 evolution. Deeper insight into the influence of Sb on PSII was obtained with measurements of in vivo chlorophyll fluorescence. The donor and the acceptor sides of PSII were shown to be the target of Sb. Sb treatment induces inhibition of electron transport from Q_A^- to Q_B/Q_B^- and accumulation of P_{680}^+. $S_2(Q_AQ_B)^-$ charge recombination and oxidation by PQ9 molecules became more important in Q_A^- reoxidation as the electron transfer in PSII was inhibited. Sb exposure caused a steady increase in the proportion of $PSII_X$ and $PSII_\beta$. These changes resulted in increased fluxes of dissipated energy and decreased index of photosynthesis performance, of maximum quantum yield, and of the overall photosynthetic driving force of PSII.

Keywords *Synechocystis* sp. · Antimony · Photosystem II · In vivo chlorophyll fluorescence

D. Zhang
State Key Laboratory of Environmental Geochemistry,
Institute of Geochemistry, Chinese Academy of Sciences,
Guiyang,
Guizhou 550002, China

X. Pan (✉) · G. Mu
Key Laboratory of Biogeography and Bioresource in Arid Land,
Xinjiang Institute of Ecology and Geography,
Chinese Academy of Sciences,
Urumqi,
Xinjiang 830011, China
e-mail: panxl@ms.xjb.ac.cn

J. Wang
Institute of Nuclear Energy, Tsinghua University,
Beijing 100083, China

Introduction

Antimony (Sb) has a molecular weight of 121.76; an atomic number of 51. Sb is a metal present in trace amount in the Earth's crust (<1.0 mg kg^{-1} of soil). It exists in a variety of oxidation states (−3, 0, 3, 5) and mainly in 3 and 5 in soil, water, biological, and mineral samples. Valentinite, stibnite, and antimnite are the main minerals containing Sb in nature. Sb is also commonly found in ores of copper, silver, lead, and coal. Huge amounts of Sb-containing compounds are annually released in the environment because of the exploitation of Sb-bearing ores. In southwestern China, where over 80% of the world's Sb ores are stored, the contamination of soil and water is a serious problem. It has been reported that Sb content in topsoil in the mining area reaches values of up to 5045 mg kg^{-1} (He et al. 2002). The concentrations of Sb in wastewater, river waters, and polluted well water are approximately 1.33–21.79, 0.063–0.037, and 24.02–42.03 mg L^{-1}, respectively (He and Yang 1999). Volcanic eruption, rock weathering, and soil runoff are also responsible for Sb emissions into the environment (Hinkley et al. 1999). Sb is widely used in various industries as integrated circuits and optoelectronic devices in the semiconductor industry (Bustamante et al. 1997), catalyst in the manufacture of polyethylene terephthalate, component of brake linings (as S_3Sb_2), as well as cable covering, ammunition flame retardant in adhesives, papers, rubber, and textiles (Smichowski 2007). Given its large utilization, large amounts of Sb-containing compounds are released into the environment. Shotyk et al. (2004) reported that Sb is the most highly enriched element in urban dusts due to the wide use of brake pads containing Sb in vehicles. Detection of Sb in snow and ice core in high arctic area indicates that Sb is a global emergent pollutant (Smichowski 2007).

Sb is potentially toxic at very low concentrations. Its toxicity is relevant to its species. Elemental Sb is more toxic than its salts, and inorganic species of Sb are more toxic than the organic ones (Smichowski 2007). Sb(III) compounds are about ten times more toxic than the Sb(V) specie. Sufficient evidence from experimental animals showed that Sb trioxide is carcinogenic. Because of this, Sb was listed as a priority pollutant by the US Environmental Protection Agency (1979) and the Council of the European Communities (1976). Sb is also on the list of hazardous substances under the Basel convention concerning the restriction of transfer of hazardous waste across borders (United Nations Environmental Program 1999).

Most studies on toxic effects of Sb arose from drug toxicology due to the wide use of Sb-containing drugs. An exposure to trivalent forms of Sb led to liver damage, hemolysis, hematuria, apoptosis in human fibroblasts, sister chromatid exchanges, a human bronchial epithelial cell line (BES-6), and circulatory disease (Huang et al. 1998). However, the knowledge on toxicological effects of Sb on aquatic organisms, microorganisms, and higher plants is still limited. Only one study we found showed that soil algae in soil were affected by Sb concentrations over 125 mg kg^{-1} soil (Hammel et al. 2000). Aquatic algae are the main primary producers and play an important role in food chains in aquatic ecosystems. In the present study, the toxicological effects of Sb (in the form of antimony potassium tartrate) on growth and photosynthesis of *Synechocystis* sp. has been investigated through the measurements of in vivo chlorophyll fluorescence.

Materials and methods

Synechocystis sp. was obtained from the Institute of Hydrobiology, Chinese Academy of Sciences and grown in BG-11 medium (Stanier et al. 1971) at 30°C under fluorescent white light (55 μmol photons $m^{-2}s^{-1}$). The growth of cultures was monitored every 12 h by measuring cell optical density at 625 nm (OD_{625}). The growth phases of algological cultures were determined using a graphical method. The cells were harvested in exponential growth phase and then transferred to 10×10-mm plastic cuvettes filled with Sb-bearing BG-11 medium at 15 μg chlorophyll mL^{-1}.

Sb treatment Sb was applied in the form of analytical-grade antimony potassium tartrate. The suspension in each cuvette was diluted to the same Chl density by addition of Sb solution and/or BG-11 medium, and the final Sb concentrations ranged from 0, 1.0, 2.5, 5.0, and 10.0 mg L^{-1}. A sample without Sb was used as the control. All the samples untreated and treated with Sb were kept in suspension by stirring and incubated at 30°C under fluorescent white light (55 μmol photons $m^{-2}s^{-1}$).

Measurement of O_2 evolution After 24 h of Sb treatment, evolution photosynthetic O_2 was measured in 2-mL cuvettes for 5 min at 25°C with a Clark microelectrode (Unisense, Denmark) under illumination with white light (500 μmol photons $m^{-2}s^{-1}$).

Chlorophyll fluorescence kinetics Chlorophyll fluorescence kinetics were measured in a dual-modulation kinetic fluorometer (FL-3500, PSI, Czech Republic). All samples were adapted to the dark for 3 min. The chlorophyll fluorescence transients were recorded up to 1 s on a logarithmic timescale. Data were acquired every 10 μs for the first 2 ms and every 1 ms thereafter. The polyphasic fluorescence induction kinetics was analyzed according to the JIP test. The polyphasic fast-phase fluorescence induction curve provides valuable information on photosystem II (PSII) function (Strasser and Govindjee 1992). In the present study, the following data were directly obtained from the fast-rise kinetic curves: F_0 (initial fluorescence) was measured at 50 μs, when all PSII reaction centers (RCs) are open; F_J and F_I are the fluorescence intensity at step J (2 ms) and at step I (30 ms), respectively; F_M (maximal fluorescence) is the peak of fluorescence at the step P when all RCs are closed; F_{300} is the fluorescence at 300 μs. Selected parameters quantifying PSII behavior were calculated from the above original data as referred in Table 1 (Strasser et al. 2000).

Q_A^- reoxidation kinetics were done in the 150 μs–10 s time range with eight fluorescence measurements taken every decade. Both actinic (25 μs) flashes and measuring (2.5 μs) flashes were provided by red LEDs. The samples at 15 μg chlorophyll mL^{-1} were dark-adapted for 3 min prior to measurement. As found through curve fitting, the reoxidation kinetics can be satisfactorily described by a sum of three independent, simultaneous exponential equations:

$$F(t) - F_0 = A_1\exp(-t/T_1) + A_2\exp(-t/T_2) + A_3\exp(-t/T_3)$$

where F(t) is the variable fluorescence yield at time *t*; F_0 is the fluorescence level before the flash; A_1–A_3 are the amplitudes; and T_1–T_3 are the time constants The nonlinear correlation between the fluorescence yield and the redox state of Q_A was corrected for using the Joliot model (Joliot and Joliot 1964) with a value of 0.5 for the energy transfer parameter between PSII units.

The proportion of $PSII_A$ and $PSII_X$ was calculated from Q_A^- reoxidation kinetics induced by a single saturating flash. The fast fluorescence decay within 50 ms represents the $PSII_A$ centers, which turn over at rates of a few hundred

Table 1 Formulae and terms used in the JIP test (Strasser et al. 2000)

Formulae and terms	Illustrations
$V_J = (F_{2ms} - F_O)/(F_M - F_O)$	Relative variable fluorescence intensity at the J-step
$M_O = 4(F_{300\mu s} - F_O)/(F_m - F_O)$	Approximated initial slope of the fluorescence transient
Quantum efficiencies or flux ratios	
$\varphi_{Po} = TR_O/ABS = [1 - (F_O/F_M)] = F_V/F_M$	Maximum quantum yield for primary photochemistry (at t=0)
$\varphi_{Eo} = ET_O/ABS = [1 - (F_O/F_M)] \bullet \Psi_O$	Quantum yield for electron transport (at t=0)
$\Psi_O = ET_O/TR_O = (1 - V_J)$	Probability that a trapped exciton moves an electron into the electron transport chain beyond QA (at t=0)
Specific fluxes or specific activities	
$ABS/RC = M_O \bullet (1/V_J) \bullet (1/\varphi_{Po})$	Absorption flux per RC
$TR_O/RC = M_O \bullet (1/V_J)$	Trapped energy flux per RC (at t=0)
$ET_O/RC = M_O \bullet (1/V_J) \bullet \Psi_O$	Electron transport flux per RC (at t=0)
$DI_O/RC = (ABS/RC) - (TR_O/RC)$	Dissipated energy flux per RC (at t=0)
Phenomenological fluxes or phenomenological activities	
$ABS/CS = ABS/CS_{Chl} = Chl/CS$	Absorption flux per CS (at t=0)
$TR_O/CS = \varphi_{Po} \bullet (ABS/CS)$	Trapped energy flux per CS
$ET_O/CS = \varphi_{Po} \bullet \Psi_O \bullet (ABS/CS)$	Electron transport flux per CS
$DI_O/CS = (ABS/CS) - (TR_O/CS)$	Dissipated energy flux per CS
Density of reaction centers	
$RC/CS = \varphi_{Po} \bullet (V_J/Mo) \bullet ABS/CS$	Density of RCs (QA-reducing PSII reaction centers)
Performance indexes	
$PI_{ABS} = (RC/ABS) \bullet [\varphi_{Po}/(1 - \varphi_{Po})] \bullet [\Psi_O/(1 - \Psi_O)]$	Performance index on absorption basis
$PI_{CS} = (RC/CS_O) \bullet [\varphi_{Po}/(1 - \varphi_{Po})] \bullet [\Psi_O/(1 - \Psi_O)]$	Performance index on cross section basis (at t=0)

electrons per second in saturating light; the slower fluorescence decay to zero represents the $PSII_X$ centers, which turn over at a rate of 1/10th to1/1,000th that of active centers due to the slow reoxidation rate of Q_A^- (Chylla and Whitmarsh 1989).

To further accurately determine the proportion of $PSII_X$, S-state tests were performed. S-state test is based on the fact that fluorescence decay is controlled largely by the reoxidation kinetics of Q_A^-. In $PSII_A$ centers, the oxidation of Q_A^- is rapid (a few milliseconds or faster), whereas in $PSII_X$ centers, the oxidation of Q_A^- is much slower (Chylla and Whitmarsh 1989; Lavergne and Leci 1993). The contribution of $PSII_X$ centers to the slow fluorescence decay is independent of flash number. To measure the proportion of inactive centers ($PSII_X$), four single turnover flashes, every 100 ms, were applied with fluorescence measurements every 200 μs. The difference between the fluorescence intensity measured at 100 ms after the fourth flash and F_0 was used to calculate the proportion of $PSII_X$ (Lavergne and Leci 1993) because the fluorescence decline after the fourth flash was mainly controlled by inactive centers, and only a small number of active centers contribute to the slow decay (Kaftan et al. 1999).

The heterogeneity of PSII antenna size ($PSII_\alpha$ and $PSII_\beta$) can be analyzed by flash fluorescence induction (Nedbal et al. 1999). $PSII_\alpha$ part is attributed to interconnected groups of PSII units that can transfer excitation energy among themselves, whereas the $PSII_\beta$ part is ascribed to individual separate PSII units that could not transfer energy to other PSII units (Melis and Homann 1976). The photosystem with high proportion of $PSII_\beta$ has low photosynthesis activity and vice versa. To study the effect of Sb on the PSII α:β heterogeneity, the flash induction test was performed (Nedbal et al. 1999). A strong 50-μs flash was applied. The proportion of $PSII_\alpha$ and $PSII_\beta$ was calculated by calculating the semilog plot of complementary area over the fluorescence induction curve (Melis and Homann 1976). Two kinetic components can be shown by the semilog plot of the area growth with fast sigmoidal component ascribed as $PSII_\alpha$ and a slow exponential component ascribed as $PSII_\beta$, respectively (Warren et al. 1983). The intercept of the linear phase in the semilog plots was denoted as the proportion of $PSII_\beta$.

Statistics Each experiment was triplicated, and the results are presented as mean or mean ± SD (standard deviation). Student's t test was used for statistical analysis of experimental data. Statistical significance was accepted when the probability of the result assuming the null hypothesis (p) is ≤0.05.

Results

Figure 1 shows that the treatment with Sb inhibits O_2 evolution of *Synechocystis* sp. The reduction is of 71.2% when the cells were exposed to 10.0 mg L^{-1} Sb for 24 h.

Fast-rise chlorophyll fluorescence kinetics Fluorescence induction kinetics of chlorophyll in cells treated with Sb for 24 h show a decrease of fluorescence intensity at increasing Sb concentration (Fig. 2a). It was found that the effect of Sb on the polyphasic fast-phase fluorescence induction curve is concentration dependent. The increasing ascending slope of fluorescence to "J" point observed in Sb-treated cells suggested that Sb slowed down electron transport from Q_A^- to Q_B and subsequent Q_A^- accumulation. The F_M value decreased, and the shape of J–I–P phase became flat as the Sb concentration increased. The decrease in F_M and fluorescence levels in the phases J and I was explained with the inhibition of the electron transport at the donor side of PSII. F_O/F_V increased from 1.7 for the control to 4.1 for cells treated with 10.0 mg L^{-1} Sb.

Results of the JIP test (Fig. 2b) showed that an increase of Sb concentration resulted in an increase of the effective antenna size per reaction center (ABS/RC) and a decrease in the quantum yield of electron transport (ET_O/ABS), electron transport per reaction center (ET_O/RC), and the density of the active photosynthetic reaction centers (RC/CS_O). These changes resulted in an increase in the dissipated energy flux per cross section (DI_O/CS) and the dissipated energy flux per reaction center (DI_O/RC), further decrease in the performance index (PI_{ABS}, PI_{CS}), maximum quantum yield for primary photochemistry (φ_{Po}), and finally a drop in the overall photosynthetic driving force. Kinetics of chlorophyll fluorescence of cells treated with 10 mg L^{-1} of Sb for different time was also determined. It was observed that there was slight increase in the original fluorescence with time while the fluorescence yield at phases J, I, and P declined and the J–I–P step transients almost become flattened at 12 h or longer (Fig. 3a). The JIP test (Fig. 3b) showed that up to 12 h the cells underwent a big increase (139%) in the apparent antenna size ABS/RC followed by a decrease (56%) in trapping per active reaction center (TR_O/RC), indicating that a fraction of reaction centers were inactivated. It was also found that electron transport flux per cross section (ET_O/CS), quantum yield for electron transport (ET_O/ABS), and the density of the active photosynthetic reaction centers (RC/CS_O) underwent significant decrease with prolonged Sb exposure within 12 h. For example, ET_O/ABS decreased from 0.074 before exposure to Sb to 0.023 after 12-h exposure to Sb. Energy dissipation (DI_O/CS) increased and performance index (PI_{ABS}) consequently decreased with increasing exposure time. The JIP test parameters changed slightly,

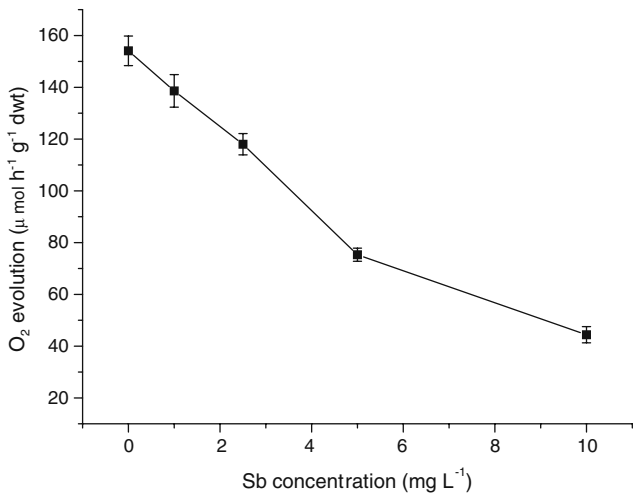

Fig. 1 Photosynthetic OBB_{2BB} evolution of *Synechocystis* sp. treated with different concentrations of Sb for 24 h. Values represent mean of three independent measurements, and *bars* indicate standard error

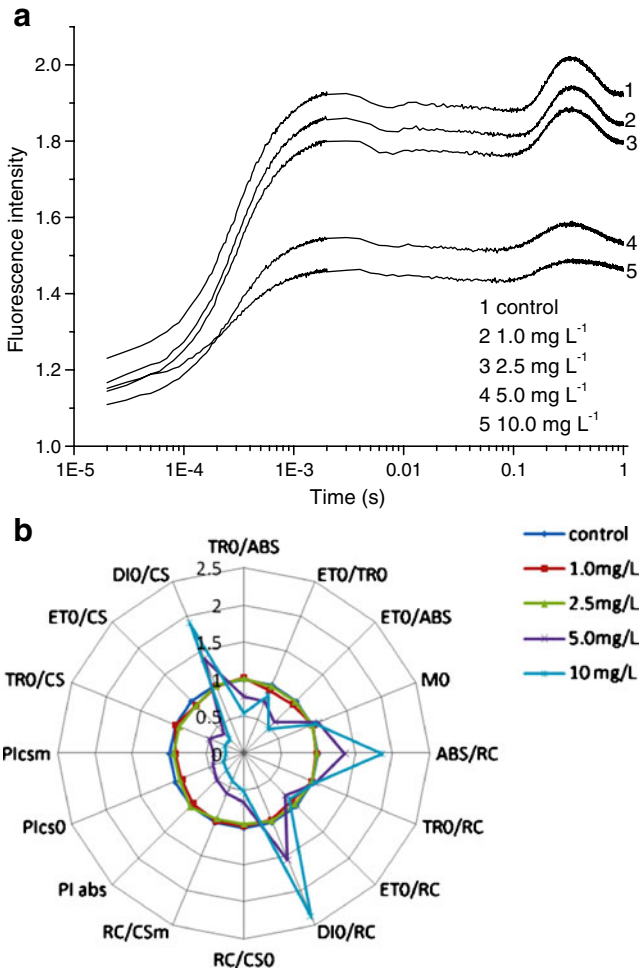

Fig. 2 **a** Representative polyphasic fast-phase fluorescence induction curve of the cell suspensions after 24-h treatment with antimony at different concentrations; **b** spider plot of parameters obtained from JIP test

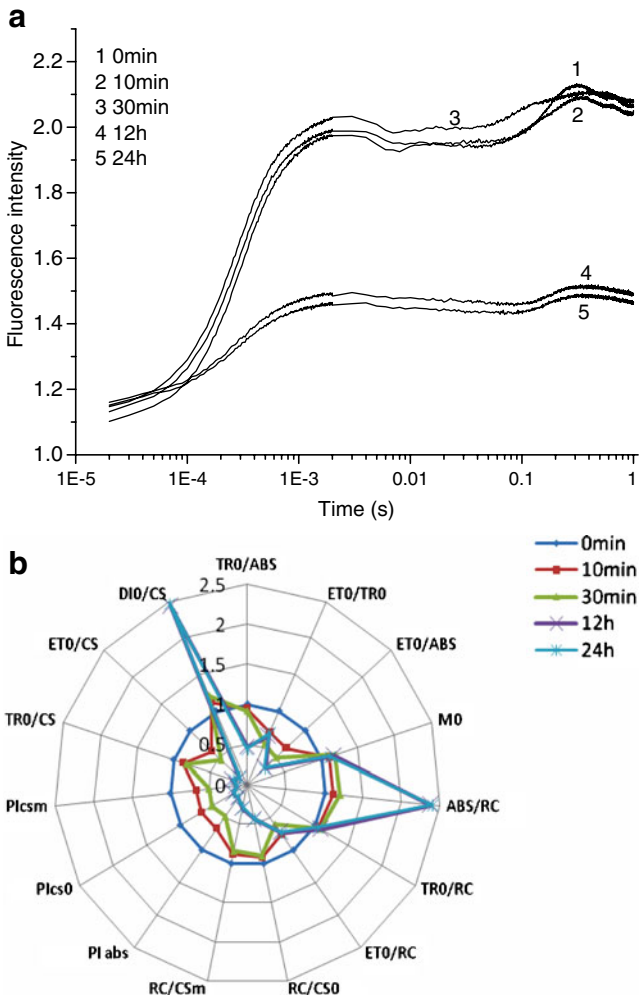

Fig. 3 **a** Representative polyphasic fast-phase fluorescence induction curve of the cells exposure to 10.0 mg/L Sb at different time; measurements of the polyphasic fast-phase fluorescence were triplicated. **b** Spider plot of parameters obtained from JIP test

and no recovery was observed within 12 and 24 h of exposure, indicating that the toxic effect on the PSII was irreversible.

Effect of Sb on Q_A^- reoxidation kinetics To investigate the effect of Sb on the functional status of the donor and acceptor sides of the PSII complex in the *Synechocystis* sp., kinetics of Q_A^- reoxidation kinetics were measured. A single turnover saturating flash to dark-adapted samples leads to a high fluorescence yield. The subsequent fluorescence decay in the dark, exhibiting three main decay phases, can be assigned to forward and backward electron transport reactions. Figure 4a shows the kinetic of Q_A^- reoxidation of control and samples treated for 24 h. The Q_A^- reoxidation kinetic parameters were summarized in Table 2. The reoxidation kinetics of both the control and Sb-treated samples were dominated by the fast phase (891.3–1231.2 μs/69.9–78.5%), which originates from Q_A^- to Q_B/Q_B^- electron transfer. It was found that the relative amplitude of the fast phase decreased, and the time needed for fast phase increased with increasing Sb concentration. For example, the amplitude of fast phase decreased from 78.5% (control) to 73.8% in samples treated with Sb at 10 mg L^{-1}, while the time constant for fast phase increased from 928.5 to 1,032.6 μs, indicating that electron transfer from Q_A^- to Q_B/Q_B^- was inhibited by Sb and that the inhibition was dependent on concentration. The relative amplitude of the slow phase (7.09–11.62 s/4.8–9.8%) arises from $S_2(Q_AQ_B)^-$ charge recombination. The relative amplitude of the slow phase substantially increased while the time constant decreased with increasing Sb concentration, indicating that the contribution of $S_2(Q_AQ_B)^-$ charge recombination to Q_A^- reoxidation correspondently increased while electron transfer from Q_A^- to Q_B/Q_B^- was severely hindered. Sb also leads to an increase in the

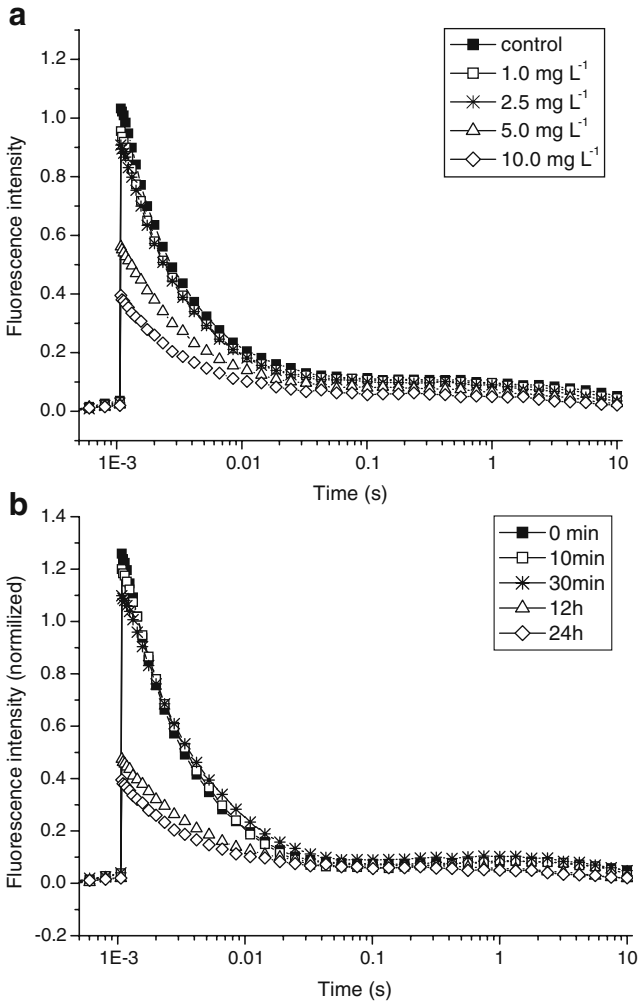

Fig. 4 **a** Representative QBB_{APBPB}^{-PP} reoxidation kinetics of the cell suspensions after 24-h treatment with different concentrations of Sb; **b** representative QBB_{APBPB}^{-PP} reoxidation kinetics of the cell suspensions treated with 10 mg LPP^{-1PP} Sb as a function of time

Table 2 Kinetic deconvolution of fluorescence decay kinetics of *Synechocystis* sp. untreated and treated with different concentrations of Sb for 24 h

Samples	Fast phase T_1 (μs)/A_1(%)	Middle phase T_2(ms)/A_2 (%)	Slow phase T_3 (s)/A_3 (%)
Control	928.5±7.9/78.5	7.96±0.22/16.7	11.62±0.65/4.8
1.0 mg L^{-1}	891.3±6.3/77.0	6.78±0.75/18.1	9.61±0.07/4.9
2.5 mg L^{-1}	992.1±7.0/75.6	7.34±0.32/19.0	7.59±0.05/5.4
5.0 mg L^{-1}	1231.2±8.1/72.9	9.76±0.21/19.0	7.16±0.03/8.1
10.0 mg L^{-1}	1032.6±5.3/69.9	9.71±0.07/20.3	7.09±0.08/9.8

Amplitudes (A_1–A_3) and time constants (T_1–T_3) were obtained by fitting the data to the three-component exponential equation. Values represent mean ± SE of three independent measurements at $p \leq 0.05$

relative amplitude of the middle phase from 16.7% for the control and 18–20.3% for Sb-treated samples. The increase in middle phase indicated that Sb increased the proportion of Q_A^- reoxidation by PQ9 molecules in PSII centers where the Q_B site was empty at the time of the flash. A decrease in F_V with increasing Sb concentration was also observed in the present study.

The time of Sb exposure on the recovery of Q_A^- reoxidation kinetics was also investigated (Fig. 4b). Exposure to Sb not only induced a decrease in the fluorescence intensity but also a decrease in the fast decaying phase in the relaxation kinetics. The parameters of Q_A^- reoxidation kinetics were summarized in Table 3. It was found that Q_A^- reoxidation kinetics rapidly responds to 10.0 mg L^{-1} Sb. The relative amplitude of fast phase rapidly decreased from 78.2% at the beginning of treatment to 68.4% after 30 min. On the contrary, as the Q_A^- to Q_B/Q_B^- electron transfer was affected, much more Q_A^- reoxidation was done by PQ9 molecules and $S_2(Q_AQ_B)^-$ charge recombination, with the relative amplitude of the middle phase and slow phase increased from 19.0% and 2.8% at the beginning to 26.4% and 5.1% at 30 min, respectively. After a longer time, the relative amplitude of the fast phase was kept at a relatively stable value (around 69%); the relative amplitude of the middle phase decreased, and the relative amplitude of the slow phase continuously increased. This suggests that within the time range from 30 min to 24 h, the electron transfer from Q_A^- to Q_B/Q_B^- was relatively stable whereas Q_A^- reoxidation via PQ9 molecules was continuously inhibited, which was compensated by an increase in the proportion of the $S_2(Q_AQ_B)^-$ charge recombination.

Effect of Sb on the active PSII centers ($PSII_A$) and inactive PSII centers ($PSII_X$) Figures 3 and 4a show that the majority (over 80%) of the Q_A^- reoxidation within 50 ms was a result of $PSII_A$ centers for the control and Sb-treated cells. Addition of Sb resulted in an increase of the percentage of $PSII_X$ and a decrease of $PSII_A$ in the total PSII centers, indicating that more and more Q_B cannot accept electrons from Q_A^-. Exposure to Sb at lower concentrations (2.5 mg L^{-1} or below) for 24 h slightly increased the proportion of $PSII_X$ centers (Fig. 5a). However, as the Sb concentration increased, the percentage of $PSII_X$ centers increased as well. For example, the percentage of $PSII_X$ increased from 6.5% for the control to 15.9% for the cells treated with 10.0 mg L^{-1} Sb for 24 h. An examination of the percentage of $PSII_X$ as a function of time showed that the percentage of $PSII_X$ centers increased from 6.1% at the beginning to 15.9% after 24 h of treatment with 10.0 mg L^{-1} Sb (Fig. 5b).

Figure 6a shows the S-state test done by a series of four flashes given 100 ms apart for the control and the samples treated with Sb at a variety of concentrations. The number of $PSII_X$ increased linearly on increase of the Sb concentration (Fig. 6b), indicating that the proportion of Q_B that cannot oxidize Q_A^- increased. For example, the number of $PSII_X$ of the control was 0.0358 and increased to 0.0549 in the presence of 10 mg L^{-1} Sb for 24 h. It also can be seen

Table 3 Kinetic deconvolution of fluorescence decay kinetics of *Synechocystis* sp. treated with 10 mg L^{-1} as a function of time

Time	Fast phase T_1 (μs)/A_1 (%)	Middle phase T_2 (ms)/A_2 (%)	Slow phase T_3 (s)/A_3 (%)
0 min	949.7±5.1 /78.2	7.09±0.21/19.0	26.92±0.74/2.8
10 min	1,095.2±7.23 /72.1	6.84±0.05/24.8	32.19±1.02/3.1
30 min	1,242.5±11.9/68.4	8.38±0.06/26.4	16.95±0.06/5.1
12 h	1,126.6±6.4/69.6	9.17±0.13/22.0	6.22±0.15/8.4
24 h	1,032.6±5.3/69.9	9.71±0.07/20.3	7.09±0.32/9.8

Amplitudes (A_1–A_3) and time constants (T_1–T_3) were obtained fitting the data with three-component exponential equation. Values represent mean ± SE of three independent measurements

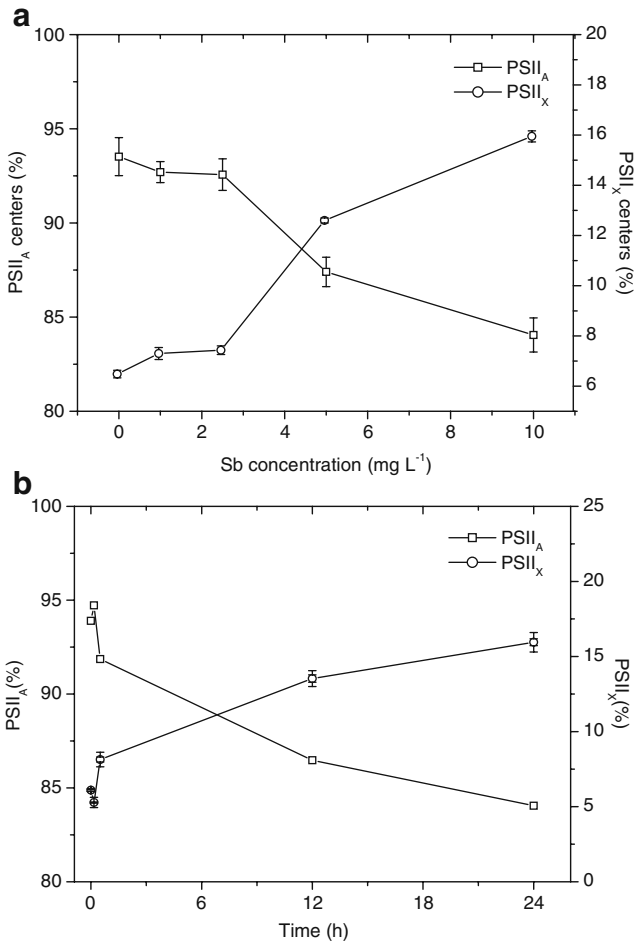

Fig. 5 **a** Change of PSIIA and PSII$_X$ of the cells after 24-h treatment with different concentrations of Sb; **b** change of PSIIA and PSII$_X$ of the cells treated with 10.0 mg LPP^{-1PP} Sb for different time. Values represent mean of three independent measurements, and *bars* indicate standard error

from Fig. 6c, d that the composition of PSII$_A$ and PSII$_X$ responded rapidly to Sb exposure. In the presence of 10 mg L^{-1} Sb, the number of PSII$_X$ centers rapidly increased from 0.0019 at the beginning to 0.0128 after 30 min. The number of PSII$_X$ centers increased linearly with prolonged exposure time. The proportion of PSII$_X$ centers at 12 and 24 h were 0.033 and 0.055, respectively.

Effect of Sb on heterogeneity of PSII antenna size In the present study, it was found that proportion of PSII$_\beta$ centers increased dramatically during Sb treatment (Table 4). PSII$_\beta$ centers accounted for about 20.15% of the PSII centers in the control and the effective antenna size of PSII$_\alpha$ was about three times larger than that of PSII$_\beta$. An increase in the Sb concentration led to a steady increase in the proportion of PSII$_\beta$. When the cells were incubated with 10.0 mg L^{-1} Sb for 24 h, the proportion of PSII$_\beta$ centers increased to 59.2%, nearly triple that of the initial. The PSII centers of *Synechocystis* sp. also responded to Sb rapidly (Table.4). For example, exposure to 10.0 mg L^{-1} Sb for 30 min led to about 5.4% increase of PSII$_\beta$.

Discussion

Effect of Sb on O_2 evolution of Synechocystis sp. In the present study, we have investigated the response of PSII of *Synechocystis* sp. to Sb treatment (antimony potassium tartrate). It is clearly shown that O_2 evolution of *Synechocystis* sp. was highly susceptible to Sb. During exposure to Sb, O_2 evolution was decreased, indicating that the O_2 evolution complex was one of the targets of Sb. It is known that PSII is the primary target of heavy metal inhibition and either the donor side or acceptor side of PSII could be the site of heavy metal (Fernades and Henriques 1991; Baron et al. 1995; Maksymiec 1997; Vrettos et al. 2001; Paddock et al. 2003). To obtain deeper insight into the mechanisms involved in influence of Sb on PSII, a variety of in vivo chlorophyll fluorescence tests were used.

Effect of Sb on the polyphasic rise chlorophyll fluorescence transient Exposure to Sb at mg L^{-1} has significant effect on the polyphasic rise chlorophyll fluorescence transient. F_M decreased and the shape of J–I–P phase became flat as the Sb concentration increased, indicating that PSII were partially inactivated and could not be closed, and the reduction of PQ (nonphotochemical phase) was inhibited (Strasser et al. 1995). The decrease in F_M and fluorescence levels in the phases J and I was explained with the inhibition of the electron transport at the donor side of PSII, which resulted in the accumulation of P_{680}^+, a strong fluorescence quencher (Govindjee 1995). The quenching effect of the variable fluorescence yield at J, I, and P was also ascribed to the deterioration of the water-splitting system (Strasser 1997). Moreover, the progressive and drastic increase in F_O/F_V with Sb concentration suggests that the severe impact of Sb on the water-splitting site probably resulted from replacement of manganese (Mn) from the water-splitting apparatus of the oxidizing side with Sb (Sayed 1998; Nirupama and Mohn 2003).

Effect of Sb on electron transport in PSII The JIP test can provide information about the fluxes of photons, excitons, electrons, and further metabolic events and has proven to be a sensitive probe for PSII behavior under environmental stress (Appenroth et al. 2001; Han et al. 2007). In this study, JIP test shows that Sb led to decrease in rate of electron transport (ET_O/ABS and ET_O/RC). An increase of V_J suggests that Sb inhibits electron transfer from Q_A^- to Q_B and subsequently results in accumulation of Q_A^-. This is in accordance with an

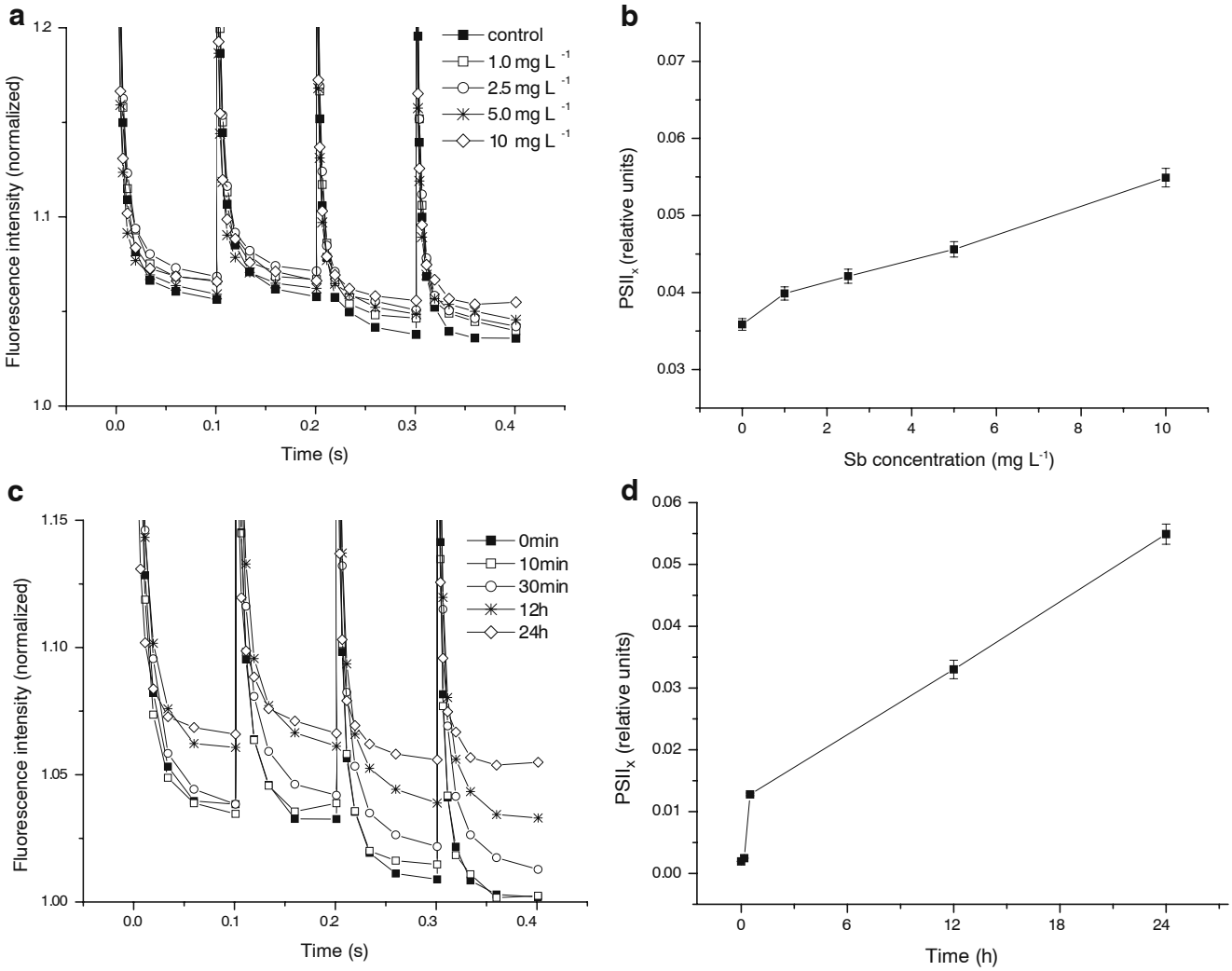

Fig. 6 **a** S-state curves of the control and samples treated with Sb at different concentrations; the curves were normalized to FBB_{0BB}. **b** Proportion of $PSII_X$ of the sample incubated with Sb (10 mg L^{-1}) as a function of Sb concentration; values represent mean of three independent measurements, and *bars* indicate standard error. **c** S-state curves of the sample incubated with Sb (10 mg L^{-1}) for different time; the curves were normalized to FBB_{0BB}. **d** Proportion of $PSII_X$ of the sample incubated with Sb (10 mg L^{-1}) as a function of time; values represent mean of three independent measurements, and *bars* indicate standard error

increase of the proportion of $PSII_X$ centers, where Q_B cannot oxidize Q_A^-, as observed in the Q_A^- reoxidation kinetics. A big decrease of F_M and flattening of J–I–P phases during exposure to higher concentration Sb showed that some PSII centers were inactivated and could not be closed due to inhibition of the electron transport at the donor side of PSII and accumulation of P_{680}^+, a strong fluorescence quencher (Govindjee 1995). Accumulation of P_{680}^+ led to inactivation of PSII centers, as confirmed by the decrease of fluorescence at 684 nm and the increase of the number of the $PSII_X$ centers in the S-state test. The inhibiting effect of Sb on electron transport in a photosystem was similar to that of

Table 4 Effect of Sb treatment on the percentage of $PSII_\beta$

	Change of the $PSII_\beta$ (%) with Sb concentration after 24h					Change of the $PSII_\beta$ (%) with time in the presence of 10.0 mg L^{-1} Sb				
Samples	Control	1.0 mg L^{-1}	2.5 mg L^{-1}	5.0 mg L^{-1}	10.0 mg L^{-1}	0 min	10 min	30 min	12 h	24 h
$PSII_\beta$ (%)	20.15±0.76	24.84±1.10	27.33±0.98	32.01±1.42	59.15±2.29	18.65±0.52	20.18±0.63	24.03±0.75	38.23±1.61	59.15±2.29

Values represent mean ± SE of three independent measurements

Cu^{2+} (Horton and Bowyer 1990; Perales-Vela et al. 2007) and Cd^{2+}(Sigfridsson et al. 2004). The Q_A^- reoxidation kinetics test confirmed the result of JIP test that electron transfer from Q_A^- to Q_B/Q_B^- was inhibited by Sb. The increase in middle phase indicated that Sb increased the proportion of Q_A^- reoxidation by PQ9 molecules in PSII centers where the Q_B site was empty at the time of the flash. Sigfridsson et al. (2004) reported a similar inhibitory effect on PSII after Cd treatments. A decrease in F_V with increasing Sb concentration was also observed in the present study, indicating that part of Q_A^- was oxidized prior to recording by the fluorometer due to faster forward electron transfer or faster recombination to P_{680}^+ remaining on the donor side of PSII after the flash (Sigfridsson et al. 2004). This method further revealed that once electron transfer from Q_A^- to Q_B/Q_B^- was inhibited by Sb, more Q_A^- was reoxidized via $S_2(Q_AQ_B)^-$ charge recombination and PQ9 molecules.

Effect of Sb on heterogeneity of PSII Q_A^- reoxidation kinetics also showed that Sb exposure caused an increase of $PSII_X$ and loss of $PSII_A$. This agrees with the decrease of the density of the active photosynthetic reaction centers (RC/CS_O). Decrease in the electron transport rate and increase in the proportion of inactivated $PSII_X$ forced PSII to regulate its light harvesting system in order to keep light energy balance between absorption and utilization so as to minimize the potential for photooxidative damage (Muller et al. 2001). Therefore, the heterogeneity of antenna size was analyzed. The JIP test revealed that Sb treatment increased the effective antenna size per reaction center (ABS/RC). The flash induction test also showed an increase of $PSII_\beta$. Accumulation of $PSII_\beta$ under stress was attributed to a decrease in the size of PSII LHCs and smaller LHCs would limit the amount of light energy that reaches PSII reaction centers, thereby protecting them from further damage (Melis and Homann 1976; Dau 1994; Pastenes and Horton 1996; Bukhov and Carpentier 2000). Accumulation of $PSII_\beta$ has also been reported to occur in higher plants following heat treatment (Guenther and Melis 1990; Melis 1991). In the present study, the result of the JIP test seems to support this explanation. The increase of the effective antenna size per reaction center (ABS/RC) could be the result of the accumulation of $PSII_\beta$ with smaller LHCs. To protect them from damage (i.e., to avoid being overexcited), the $PSII_\beta$ LHCs decreased the TR_O/ABS. As a result of the accumulation of $PSII_\beta$, the interconnectivity between PSII units became worse and the excitation energy transfer between them was inhibited, which resulted in an increase of energy dissipation (DI_O/CS_O).

Change of $PSII_\beta$ during exposure to Sb showed the same trend, indicating that there are some common properties between $PSII_X$ and $PSII_\beta$. However, the proportion of $PSII_\beta$ exceeded that of $PSII_X$ at all times, which means that they are not identical and $PSII_X$ was possibly a part of $PSII_\beta$. In other words, there are some $PSII_A$ centers where Q_B was capable of accepting electrons from Q_A^- but with smaller peripheral LHCs ($PSII_\beta$; Oxborough et al. 1996).

In conclusion, we observed a drastic inhibitory effect on PSII of *Synechocystis* sp. during exposure to Sb (1.0–10.0 mg L^{-1}). Sb inhibited PSII in the following aspects.

(1) Sb decreases O_2 evolution, fluorescence yield at 684 nm, maximum quantum yield for primary photochemistry, and damages cellular compounds;
(2) the site of Sb inhibition was on both PSII donor side and acceptor side. Sb exposure resulted in an inhibition of electron transport from Q_A^- to Q_B/Q_B^- and accumulation of P_{680}^+;
(3) Under Sb stress, Q_A^-reoxidation turned more to $S_2(Q_AQ_B)^-$ charge recombination and oxidation by PQ9 molecules;
(4) Sb exposure steadily increased the proportion of $PSII_X$ and $PSII_\beta$;
(5) the above changes finally resulted in an increase of dissipated energy flux and decrease in the performance index (PI_{ABS}, PI_{CS}), maximum quantum yield for primary photochemistry(ϕP_O), and the overall photosynthetic driving force.

Our results demonstrate that the JIP test, S-state test, Q_A^- reoxidation kinetic test, and flash induction test are useful for studying the toxic effects of pollutants on photosynthetic organisms.

Acknowledgements This work was supported by Knowledge Innovation Program of Chinese Academy of Sciences (KZCX2-YW-335 and KZCX2-YW-135), Program of 100 Distinguished Young Scientists of the Chinese Academy of Sciences, National Natural Science Foundation of China (40673070, 40872169) and 863 program project 2006AA06Z339 from MOST of China. We are grateful to the editor and the anonymous reviewers for their valuable comments and suggestions.

References

Appenroth KJ, Stockel J, Srivastava A, Strasser RJ (2001) Multiple effects of chromate on the photosynthetic apparatus of *Spirodela polyrhiza* as probed by OJIP chlorophyll *a* fluorescence measurements. Environ Poll 115:49–64

Baron M, Arellano JB, Gorge LJ (1995) Copper and photosystem II: a controversial relationship. Physiol Plant 94:174–180

Bukhov NG, Carpentier R (2000) Heterogeneity of photosystem II reaction centres as influenced by heat treatment of barley leaves. Physiol Plant 110:279–285

Bustamante J, Lennart D, Marie V, Bruce F, Sten O (1997) The semiconductor elements arsenic and indium induce apoptosis in rat thymocytes. Toxicology 118:129–136

Chylla RA, Whitmarsh J (1989) Inactive photosystem II complexes in leaves. Turnover rate and quantitation. Plant Physiol 90:765–772

Council of the European Communities (1976) Council Directive 76/464/EEC of 4 May 1976 on pollution caused by certain dangerous

substances discharged into the aquatic environment of the Community. Official Journal L 129, 18 May 1976, pp. 23–29.
Dau H (1994) Molecular mechanisms and quantitative models of variable photosystem II fluorescence. Photochem Photobiol 60:1–23
Fernades JC, Henriques FS (1991) Biochemical, physiological and structural effects of excess copper in plants. Bot Rev 57:246–273
Govindjee (1995) Sixty-three years since Kautsky: chlorophyll a fluorescence. Aust J Plant Physiol 34:1073–1079
Guenther JE, Melis A (1990) The physiological significance of photosystem II heterogeneity in chloroplasts. Photosynth Res 23:105–109
Hammel W, Debus R, Steubing L (2000) Mobility of antimony in soil and its availability to plants. Chemosphere 41:1791–1798
Han T, Kang S-H, Park J-S, Lee H-K, Brown MT (2007) Physiological responses of *Ulva pertusa* and *U. armoricana* to copper exposure. Aquat Toxicol. doi:10.1016/j.aquatox.2007.10.016
He MC, Yang JR (1999) Effects of different forms of antimony on rice during the period of germination and growth and antimony concentration in rice tissue. Sci Total Environ 243–244:149–155
He MC, Ji HB, Zhao CY, Xie J, Wu XM, Li ZF (2002) Preliminary studies of heavy metal pollution in soil and plant near antimony mine area. J Beijing Normal University (Nat Sci) 38:417–420
Hinkley TK, Lamothe PJ, Wilson SA, David L, Finnegan TM, Gerlach TM (1999) Metal emissions from Kilauea, and a suggested revision of the estimated worldwide metal output by quiescent degassing of volcanoes. Earth Planet Sci Lett 170:315–325
Horton P, Bowyer TR (1990) Chlorophyll fluorescence transients. In: Harwood JL, Bowyer TR (eds) Methods in plant biochemistry. Lipids, membranes and aspects of photobiology. Academic, San Diego, pp 259–295
Huang H, Shu SC, Shih JH, Kuo CJ, Chiu ID (1998) Antimony trichloride induces DNA damage and apoptosis in mammalian cells. Toxicology 129:113–123
Joliot A, Joliot P (1964) Etude cine tique de la reaction photochimique liberant loxygene au cours de la photosynthese. C R Acad Sci 258:4622–4625
Kaftan D, Meszaros T, Whitmarsh J, Nedbal L (1999) Characterization of photosystem II activity and heterogeneity during the cell cycle of the green alga *Scenedesmus quadricauda*. Plant Physiol 120:433–441
Lavergne J, Leci E (1993) Properties of inactive photosystem II centers. Photosynth Res 35:323–343
Maksymiec W (1997) Effect of copper on cellular processes in higher plants. Photosynthetica 34:321–342
Melis A (1991) Dynamics of photosynthetic membrane composition and function. Biochim Biophys Acta 1058:87–106
Melis A, Homann PH (1976) Heterogeneity of the photochemical centers in system II of chloroplasts. Photochem Photobiol 23:343–350
Muller P, Xiao-Ping L, Niyogi KK (2001) Non-photochemical quenching: a response to excess light energy. Plant Physiol 125:1158–1566
Nedbal L, Trtílek M, Kaftan D (1999) Flash fluorescence induction: a novel method to study regulation of photosystem II. J Photochem Photobiol B Biol 48:154–157
Nirupama M, Mohn FH (2003) Use of chlorophyll fluorescence in metal-stress research: a case study with the green microalga *Scenedesmus*. Ecotox Env Safety 55:64–69
Oxborough K, Nedbal L, Chylla RA, Whitmarsh J (1996) Light dependent modification of photosystem II in spinach leaves. Photosynth Res 48:247–254
Paddock ML, Sagle L, Tehrani A, Beatty JT, Feher G, Okamura MY (2003) Mechanism of proton transfer inhibition by Cd^{2+} binding to bacterial reaction centers: determination of the pK(A) of functionally important histidine residues. Biochemistry 42:9626–9632
Pastenes C, Horton P (1996) Effect of high temperature on photosynthesis in beans. I. Oxygen evolution and chlorophyll fluorescence. Plant Physiol 112:1245–1251
Perales-Vela HV, Gonzalez-Moreno S, Montes-Horcasitas C, Canizares-Villanueva RO (2007) Growth, photosynthetic and respiratory responses to sub-lethal copper concentrations in *Scenedesmus incrassatulus* (Chlorophyceae). Chemosphere 67:2274–2281
Sayed OH (1998) Analysis of photosynthetic responses and adaptation to nitrogen starvation in *Chlorella* using in vivo chlorophyll fluorescence. Photosynthetica 35:611–619
Shotyk W, Krachler M, Chen B (2004) Antimony in recent peat from Switzerland and Scotland: comparison with natural background values (5,320 to 8,020 14C yr BP), correlation with Pb, and implications for the global atmospheric Sb cycle. Global Biogeochem Cycles 18:GB1016. doi:10.1029/2003GB002113
Sigfridsson KGV, Bernat G, Mamedov F, Styring S (2004) Molecular interference of Cd^{2+} with photosystem II. Biochim Biophys Acta 1659:19–31
Smichowski P (2007) Antimony in the environment as a global pollutant: a review on analytical methodologies for its determination in atmospheric aerosols. Talanta. doi:10.1016/j.talanta11.005
Stanier RY, Kunisawa R, Mandel M, Cohen-Bazire G (1971) Purification and properties of unicellular blue–green algae (Order Chroococcales). Bacteriol Rev 35:171–205
Strasser BJ (1997) Donor side capacity of photosystem II probed by chlorophyll a fluorescence transients. Photosynth Res 52:147–155
Strasser RJ, Govindjee (1992) On the O–J–I–P fluorescence transient in leaves and D1 mutants of *Chlamydomonas reinhardtii*. In: Murata N (ed) Research in photosynthesis. Kluwer, Dordrecht, pp 29–32
Strasser RJ, Srivastava A, Govindjee (1995) Polyphasic chlorophyll a fluorescence transient in plant and cyanobacteria. Photochem Photobiol 61:32–42
Strasser RJ, Srivastava A, Tsimilli-Michael M (2000) The fluorescence transient as a tool to characterize and screen photosynthetic samples. In: Yunus M, Pathre U, Mohanty P (eds) Probing photosynthesis: mechanism. Regulation and adaptation. Taylor & Francis, London, pp 443–480
United Nations Environmental Program (1999) Basel Convention on the Control of Transboundary Movements of Hazardous Wastes and Their Disposal with amended Annex I and two additional Annexes VIII and IX, adopted at the fourth meeting of the Conference of the Parties in 1998. SBC No. 99/001. UNEP, Geneva.
United States Environmental Protection Agency (1979) Water related fate of the 129 priority pollutants, vol. 1. USEPA, Washington, DC, USA, EP-440/4-79-029A. 23–29.
Vrettos JS, Stone DA, Brudvig GW (2001) Quantifying the ion selectivity of the Ca^{2+} site in photosystem II: evidence for direct involvement of Ca^{2+} in O_2 formation. Biochemistry 40:7937–7945
Warren LB, Douglas M, Sylvia B (1983) Fluorescence lifetimes in the bipartite model of the photosynthetic apparatus with α, β heterogeneity in photosystem II. Proc. Natl. Acad. Sci. USA 80:7510–7514